MOLECULAR AND CELLULAR BIOLOGY, Sept. 1996, p. 4832–4841 Vol. 16, No. 9
0270-7306/96/$04.00+0

Human Rad50 Is Physically Associated with Human Mre11: Identification of a Conserved Multiprotein Complex Implicated in Recombinational DNA Repair†

GREGORY M. DOLGANOV,[1]* RICHARD S. MASER,[2] ALEXANDER NOVIKOV,[1] LIANA TOSTO,[1] SUSAN CHONG,[1] DEBRA A. BRESSAN,[2] AND JOHN H. J. PETRINI[2]*

Human Genome Group, Genelabs Technologies, Inc., Redwood City, California 94063,[1] and Laboratory of Genetics, University of Wisconsin Medical School, Madison, Wisconsin 53706[2]

Received 3 April 1996/Returned for modification 16 May 1996/Accepted 10 June 1996

In this report, we describe the identification and molecular characterization of a human *RAD50* homolog, *hRAD50*. *hRAD50* was included in a collection of cDNAs which were isolated by a direct cDNA selection strategy focused on the chromosomal interval spanning 5q23 to 5q31. Alterations of the 5q23-q31 interval are frequently observed in myelodysplasia and myeloid leukemia. This strategy was thus undertaken to create a detailed genetic map of that region. *Saccharomyces cerevisiae RAD50* (*ScRAD50*) is one of three yeast *RAD52* epistasis group members (*ScRAD50*, *ScMRE11*, and *ScXRS2*) in which mutations eliminate meiotic recombination but confer a hyperrecombinational phenotype in mitotic cells. The yeast Rad50, Mre11, and Xrs2 proteins appear to act in a multiprotein complex, consistent with the observation that the corresponding mutants confer essentially identical phenotypes. In this report, we demonstrate that the human Rad50 and Mre11 proteins are stably associated in a protein complex which may include three other proteins. *hRAD50* is expressed in all tissues examined, but mRNA levels are significantly higher in the testis. Other human *RAD52* epistasis group homologs exhibit this expression pattern, suggesting the involvement of human *RAD52* epistasis group proteins in meiotic recombination. Human *RAD52* epistasis group proteins are highly conserved and act in protein complexes that are analogous to those of their yeast counterparts. These findings indicate that the function of the *RAD52* epistasis group is conserved in human cells.

Acute myeloid leukemia (AML) and myelodysplastic disease are associated with alterations of the 5q23-q31 chromosomal interval (25, 60, 63). Extensive analysis of patient material has narrowed the commonly deleted region to 5q31, leading to the proposal that an AML tumor suppressor is contained within this region. This interval has thus been designated the critical region (45, 46, 60). We undertook the creation of a detailed transcriptional and physical map of the 5q23-q31 interval and used direct cDNA selection to identify potential tumor suppressors in this region (16a). Among the cDNAs isolated by this method was *hRAD50*, a human homolog of the *Saccharomyces cerevisiae* DNA repair gene, *ScRAD50*. We have mapped the *hRAD50* locus to 5q31, placing it in the critical region proposed to contain the AML tumor suppressor (45). Its homology to *ScRAD50* argues that *hRAD50* encodes a protein that is involved in human recombinational DNA repair.

Double-strand-break (DSB) repair proteins are involved in diverse DNA recombination processes in mammalian and yeast cells. In addition to conferring sensitivity to DNA-damaging agents, DSB repair deficiency affects meiotic and mitotic recombination, mating-type switching, and the assembly of antigen receptor genes (20, 86). Although defects in DSB repair and DNA recombination are coincident in both mammals and *S. cerevisiae*, the prevalent mechanisms of recombinational DNA repair differ significantly in these systems (8, 26). Nonhomologous recombination is much more frequent than homologous recombination in mammalian cells (81), whereas yeast cells rely almost entirely on homology-based recombinational DNA repair (71). Relatively few mammalian DSB repair genes have been identified, and so the basis of the strong preference for illegitimate recombination is not well understood. Recently, three genes which specify functions in mammalian DSB repair have been isolated and characterized, using rodent mutant cell lines that exhibit sensitivity to ionizing radiation (IR) (7, 22, 34, 87). The mutant genes, *xrcc4* (from the cell line XR-1), *xrcc5* or *Ku 86* (*xrs6*), and *xrcc7* or *scid* (*v3*), confer generalized DSB repair deficiency and disrupt V(D)J recombination, a site-specific illegitimate recombination process required for the assembly of antigen receptor genes (6, 9, 29, 78, 79). Characterization of these genes and the corresponding protein products has provided the first insight into the molecular basis of DSB repair in mammalian cells. At least five additional radiosensitive rodent complementation groups have been described, indicating that most genes of the mammalian DSB repair pathway have not yet been isolated (35, 37, 47, 82, 84).

The *RAD52* epistasis group is the major DSB repair pathway in *S. cerevisiae* and is composed of 10 genes (*RAD50* to *RAD57*, *MRE11*, and *XRS2*) (1, 20). Hence, the highly conserved human *RAD52* epistasis group homologs, *hRAD51*, *hRAD52*, and *hMRE11*, are also implicated in the mammalian DSB repair pathway (5, 65, 74, 75). In spite of the apparent differences between mammals and *S. cerevisiae*, the primary sequence conservation of human *RAD52* epistasis group homologs must

* Corresponding author. Mailing address for Gregory M. Dolganov: Human Genome Group, Genelabs Technologies, Inc., 505 Penobscot Dr., Redwood City, CA 94063. Phone: (415) 369-9500. Fax: (415) 368-0709. Electronic mail address: dolgreg@netcom.com. Mailing address for John H. J. Petrini: University of Wisconsin Medical School, Laboratory of Genetics, 445 Henry Mall, Madison, WI 53706. Phone: (608) 265-6043. Fax: (608) 262-2976. Electronic mail address: jpetrini@facstaff.wisc.edu.

† Paper 3461 from the University of Wisconsin Laboratory of Genetics.

reflect that certain mechanistic features of DSB repair are also conserved.

S. cerevisiae RAD52 epistasis group mutants can be divided into two subgroups on the basis of their respective mitotic recombination phenotypes. Mitotic recombination is sharply reduced by *Scrad51*, *Scrad52*, *Scrad54*, *Scrad55*, and *Scrad57* mutations (20), whereas spontaneous recombination rates are increased at least 10-fold in *Scrad50*, *Scmre11*, and *Scxrs2* mutants (1, 3, 53, 88). In contrast to other *RAD52* epistasis group mutants, *Scrad50* and *Scmre11* mutants do not exhibit overt defects in homologous recombination. These mutants are defective in nonhomologous DNA end joining and chromosomal integration, whereas mutation of *Scrad51*, *Scrad52*, *Scrad54*, or *Scrad57* does not affect these nonhomologous DNA recombination reactions (58, 71). The phenotypic similarities within each of these subgroups reflect that the proteins encoded by these loci act in multiprotein complexes. A complex containing ScRad51, ScRad52, ScRad55, and ScRad57 has been suggested by genetic and biochemical analyses (17, 28, 57, 76). Similarly, evidence for interaction of ScRad50, ScXrs2, and ScMre11 proteins has been obtained (36).

The recent identification of the human *ScMRE11* homolog, *hMRE11* (65), provides a means to assess whether a mammalian analog of the *S. cerevisiae* Rad50-Mre11-Xrs2 complex plays a role in human DSB repair. Among the three members of the yeast complex, a large number of *Scrad50* mutant alleles have been characterized (2), allowing functional and structural analysis of the yeast Rad50 protein. ScRad50 is a 153-kDa protein with heptad repeat motifs that suggest an alpha-helical coiled-coil structure similar to that of the rabbit myosin heavy chain (3, 54). Consistent with the presence of heptad repeats, purified Rad50 appears to exist as a homodimeric or oligomeric protein complex (66). ScRad50 also contains Walker A (N-terminal) and B (C-terminal) motifs that characterize a large number of ATP-binding proteins (24, 30, 85). The presence of nucleoside triphosphate (NTP) binding domains accounts for the fact that the DNA binding activity of purified ScRad50 is ATP dependent (66). Since mutations in conserved residues of the N-terminal ATP binding domain confer a null phenotype (2), the ability of ScRad50 to bind ATP, hence to bind DNA, is required for its function. The structural features of ScRad50 are shared by the recently described SMC (for structural maintenance of chromosomes) superfamily of proteins which mediate processes relevant to higher-order chromosome structure and dynamics (30, 69). The identification of the *hRAD50* locus at 5q31 suggests that recombinational DNA repair deficiency may be associated with the development of myeloid leukemia.

MATERIALS AND METHODS

Cell lines. IMR90 primary fibroblasts were maintained in Dulbecco modified Eagle medium–10% fetal calf serum–penicillin-streptomycin–2 mM L-glutamine and serially passaged 1:3 from passage 8. Experiments using IMR90 cells were performed with cells from passages 12 to 16. TK6 lymphoblastoid and K562 CML cells were grown in RPMI 1640–10% newborn calf serum–1% penicillin-streptomycin–2 mM L-glutamine. All cells were grown at 37°C in 5% CO_2. K562 cells were a gift from Peggy Farnham. IMR90 and TK6 cells were obtained from the American Type Culture Collection. HHW105, a natural human-hamster hybrid cell line containing the intact human chromosome 5 and matching CHO genomic DNA, were kindly provided by J. Wasmuth.

Isolation of cosmid and YAC clones. Isolation and analysis of cosmid, yeast artificial chromosome (YAC), and mega-YAC clones from the 5q31 chromosomal region were carried out as described previously (11, 50) and will be described in detail elsewhere (16a). A human chromosome 5-specific cosmid library was kindly provided by L. Deaven (Los Alamos National Laboratories, Los Alamos, N.Mex.) as arrayed clones in a 96-well plate format. YAC clones were isolated from either Washington University (St. Louis, Mo.) or the Centre d'Etude du Polymorphisme Humain (Paris, France) YAC libraries, using PCR on the clone pools.

TABLE 1. PCR primers used for analysis of the *hRAD50* gene

Primer	Sequence
A106-1	gtcatccagactcagagctc
A106-2	ctgtctaggcaaacatgctc
2B-8	ccaggctcactcacagagtcaagg
A106-AR	tttctatggcatttaaatcttggatattt
B4-2	ccttgttcacaagttctgttgtcctc
N6Z-1	cataattgatttgagggagaagga
N6Z-2	gtaacatctgtcaggcatactttggcact
G10-2	gcattgtggctacggcttgcgtcc
G10-14	tctaatctcaccagggacctg
G10-N	gagaggatcctttgtggactccaggtccctggtgagatt
G10-C1	gagaggatccatgaacattgaatcccagggag
A106-21	tcccttcagcatcaccactcggtag

Direct cDNA selection and DNA sequencing. Direct cDNA selection with the YACs A94G6 and 854G6 was carried out as described previously (59), with minor modifications. One hundred nanograms of the biotinylated YAC DNA was preblocked with 10 μg of Cot1 DNA in 10 μl of 5× SSPE (1× SSPE is 0.18 M NaCl, 10 mM NaH_2PO_4, and 1 mM EDTA [pH 7.7])–1× Denhardt's solution–0.1% sodium dodecyl sulfate (SDS) for 2 h at 60°C; 10 μg of denatured cDNAs derived as described above in 10 μl of the same buffer was added, and hybridization continued for 4 h at 65°C. The ensuing genomic DNA-cDNA hybrids were captured on streptavidin-coated magnetic beads and washed. cDNAs were then eluted, amplified, and recycled through an additional round of enrichment as described above.

cDNA pools were constructed by using SuperScript Choice System (Life Technologies, Inc., Gaithersburg, Md.) according to the manufacturer's protocol. RNA samples used were derived from total embryo (6, 8, and 12 weeks of gestation), fetal liver, fetal brain, fetal muscle, placenta, adult heart, adult kidney, bone marrow, and activated T and B cells and were kindly provided by A. Rynditch. Additional RNA preparations were either purchased or kindly provided by A. Chenchik, Clontech Laboratories, Inc. (Palo Alto, Calif.). One microgram of total RNA from the above-specified sources was reverse transcribed by random priming with Superscript II in 20 μl of reaction mix as specified by the manufacturer (Life Technologies).

For PCR, 1 μl of the reverse transcriptase reaction described above was used in PCR mixtures containing 20 mM Tris-HCl (pH 8.9) (at 25°C), 16.7 mM $(NH_4)_2SO_4$, 1.5 mM $MgCl_2$, 200 μM dNTPs, 1 μM primers, and 0.8 U of AmpliTaq (Cetus) in a final volume of 30 μl. Approximately 10 ng of genomic DNA was used as the template where appropriate. PCR products were analyzed by agarose gel electrophoresis after 30 cycles of conventional PCR.

The full-length *hRAD50* cDNA was derived by RACE (rapid amplification of cDNA ends), using the Marathon RACE kit (Clontech) according to manufacturer's specifications, from cDNA pools constructed as described above. Sequences of PCR primers used for analysis of the *hRAD50* are shown in Table 1.

DNA sequencing. The PCR products were subcloned into plasmid pCRTMII (Invitrogen Corporation, San Diego, Calif.) or pAMP10 (Life Technologies). In some cases, sequencing was carried out on PCR product without subcloning. Nested cDNA primers or vector-based primers (sequences not shown) were used with a DyeDeoxy terminator cycle sequencing kit, using a model 373A DNA sequencing system (Applied Biosystems, Inc., Foster City, Calif.). Sequence assembly and analysis of the full-length *hRAD50* cDNA were carried out with the ABI Factura Auto-Assembler and Sequence Navigator software packages (Applied Biosystems). DNA sequences were analyzed by using BlastN and BlastX searches of National Center for Biotechnology Information databases.

Irradiation. Cells were irradiated in a Mark I ^{137}Cs source at a rate of approximately 200 cGy/min.

Molecular biology. Plasmid construction and Northern (RNA) blotting were carried out according to standard procedures (4). The human multiple-tissue Northern blot was purchased from Clontech. Molecules were radiolabeled as described by Feinberg and Vogelstein (18) for use as hybridization probes.

Immunoblot analysis. hRad50 and hMre11 antisera (αhRad50 and αhMre11) were raised in New Zealand White rabbits by using bacterially produced histidine-tagged (hMre11) or glutathione *S*-transferase (hRad50) fusion proteins. The resulting reagents were (i) preimmune serum 204pre and immune serum 204/6 (αhMre11) and (ii) preimmune serum 84pre and immune serum 84 (αhRad50). Neither the hMre11 nor the hRad50 antiserum thus derived cross-reacts with the corresponding yeast homologs. Affinity purification αhMre11 was carried out essentially as described previously (27). Bacterially produced hMre11 was conjugated to Actigel resin (Sterogene Separations, Inc., Arcadia, Calif.). Ten milliliters of rabbit antiserum was passed over a column containing 10 ml of the resulting hMre11-conjugated resin. After extensive washing, bound antibody was eluted from the column by using Actisep elution medium (Sterogene Separations) followed by 4 M guanidine-HCl–10 mM Tris (pH 8). Elution was monitored by UV absorbance, protein fractions were dialyzed against phosphate-buffered saline (PBS), and the dialysate was concentrated to 1 mg/ml prior to use.

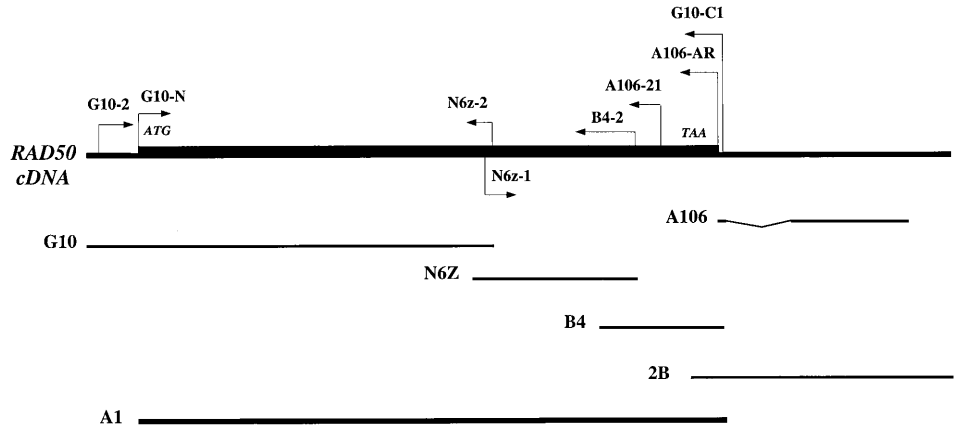

FIG. 1. Isolation and assembly of the *hRAD50* cDNA. Representative individual cDNA clones are depicted below the assembled *hRAD50* cDNA sequence by solid lines. Clone A106 is spliced. PCR primers and their orientations are depicted by arrows. The ABI Auto-Assembler software package was used to generate the *hRAD50* full-length cDNA from the individual clones. Clone A1 was generated by long-range PCR with primers G10-N and G10-C1, subcloned, and sequenced with at least twofold coverage. Clone 2B is a sequenced genomic fragment derived from cosmid 256E2, which is colinear with the cDNA sequence.

For Western blotting (immunoblotting), 0.5×10^6 to 2×10^6 cells were lysed in SDS lysis buffer containing β-mercaptoethanol, aspirated through a 25-gauge needle to shear the genomic DNA, and boiled before fractionation on SDS-polyacrylamide gels. Immunoblot analysis was carried out with the indicated antisera at dilutions of 1:400 to 1:1,000, using standard procedures (27). Chemiluminescent detection of filter-bound antigen-antibody complexes was done with horseradish peroxidase-conjugated protein G plus protein A in conjunction with Luminol reagent (Pierce, Rockford, Ill.). Where indicated, blots were stripped at 50°C for 30 min in strip buffer (62.5 mM Tris-HCl [pH 6.8], 100 mM β-mercaptoethanol, 2% SDS) and retreated with primary and secondary immunoblot reagents as described above.

Immunoprecipitation analyses. TK6 cells (2.5×10^6) were lysed on ice for 30 min in high-salt buffer (500 mM NaCl, 10 mM Tris [pH 7.5], 10 mM EDTA, 0.5% Nonidet P-40, 0.2 mg of phenylmethylsulfonyl fluoride per ml). Lysates were then diluted 1:2 with standard lysis buffer (100 mM NaCl, 50 mM Tris [pH 7.4], 5 mM EDTA, 0.5% Nonidet P-40) or with lysis buffer containing increased NaCl concentrations and precleared for 1 h at 4°C with protein A-Sepharose beads (Pharmacia, Piscataway, N.J.). Cleared lysates (final NaCl concentration, 300 mM to 1,000 mM) were incubated on ice for 1 h with hMre11 serum 204/3p (affinity-purified αhMre11), 204pre, hRad50 serum 84, or 84pre. Immune complexes were precipitated for 1 h by rolling at 4°C with protein A-Sepharose beads. Bead-bound immunoprecipitates were washed four times with standard lysis buffer, boiled in SDS sample buffer, and loaded on SDS–8.5% polyacrylamide gels. Proteins were analyzed by immunoblotting using standard methods (27) and detected as described above.

Metabolic labeling. K562 cells (5×10^6) were removed from normal medium, washed once with PBS, and resuspended in methionine- and phosphate-free RPMI 1640 supplemented with 2% dialyzed newborn calf serum, 8 mg of Na_2HPO_4 per ml, and 85 μCi of [^{35}S]methionine (10 μCi/μl) per ml. Cells were incubated for 6 h prior to harvesting for immunoprecipitation. Immunoprecipitates were fractionated on SDS–8.5% polyacrylamide gels. Gels were fixed for 30 min in 30% methanol–10% acetic acid, washed in double-distilled H_2O, and incubated in 1 M sodium salicylate for 30 min prior to drying and autoradiography. Protein bands were readily visible within 7 h.

Photography. Photographic images were scanned directly from autoradiograms or from photographs of autoradiograms by using Adobe Photoshop. In some cases, image contrast was adjusted, but otherwise unaltered images were published as editions and annotated (lane designations, etc.) by using Deneba Canvas 3.5.4.

RESULTS

Isolation of the *hRAD50* cDNA by direct cDNA selection. Direct cDNA selection was developed to allow for the rapid identification of genes within specific genomic regions (51, 59). This technique has been widely applied for positional cloning (for example, reference 19). Direct cDNA selection is achieved through hybridization of cDNA to biotinylated genomic DNA encompassing the chromosomal region of interest. cDNA molecules with homology to the particular chromosomal segment under examination are thus captured as genomic DNA-cDNA hybrids. The procedure is repeated to further enrich for region-specific cDNAs. Captured cDNAs are then eluted from genomic DNA-cDNA hybrids, PCR amplified, and subcloned for subsequent analysis. We have shown that this approach can result in 100,000-fold enrichment of cDNAs specific to a particular genomic segment (59). We carried out direct cDNA selection with two overlapping YACs, A94G6 and mega-YAC 854G6, that span approximately 1.2 Mb in the 5q23-q31 interval (16, 59). Among the isolated cDNAs, clone A106 displayed specific expression in activated T and B cells, fetal liver, thymus, ovary, and testis (data not shown). Clone A106 was used to screen the micrograddied chromosome 5-specific cosmid library. Two positive clones, 256E1 and 113E9, which we had previously identified in mapping the *IL13* gene to 5q31 (16), were obtained. DNA sequencing of the A106 cDNA and a subclone of the 256E1 cosmid clone (clone 2B [Fig. 1]) revealed homology to the C-terminal region of *ScRAD50* (3). Conventional 5′ RACE extension of the A106 cDNA clone resulted in the generation of cDNA clone B4 (Fig. 1). DNA sequence analysis of this clone revealed additional homology to the C-terminal portion of the *ScRAD50* gene, indicating that A106 and B4 partially comprised the coding sequence of *hRAD50*. Subsequent RACE extensions culminated in the isolation of the cDNA clone G10, which allowed us to assemble the full-length *hRAD50* cDNA, A1 (Fig. 1). Conceptual translation of this 5,894-bp cDNA is shown in comparison with ScRad50 (Fig. 2).

Chromosomal localization of the *hRAD50* locus. Southern blot analysis of cosmid clones 256E1, 113E9, and 58D6 placed the A106 locus approximately 14.0 kb upstream of the *IL13* gene (Fig. 3A). These cosmid clones have previously been localized to 5q31 by fluorescent in situ hybridization analysis (70). Full-length *hRAD50* cDNA (clone A1) was also used as a probe in Southern blot hybridization analysis of YACs A94G6 and 854G6. This analysis confirmed that *hRAD50* maps to the same 320-kb *Not*I restriction fragment as the *IL4*, *IL13*, and *IL5* genes (data not shown) (16, 59). Additional confirmation of this localization was established by PCR of DNA prepared from YACs A94G6 and 854G6, as well as from the chromosome 5-containing human-hamster hybrid cell line HHW105, with primers based on the 5′ *hRAD50* noncoding region. The *hRAD50* primers amplified the expected products in the YAC clones derived from 5q31 and the human-hamster hybrid cell, whereas PCR with these primers on hamster genomic DNA

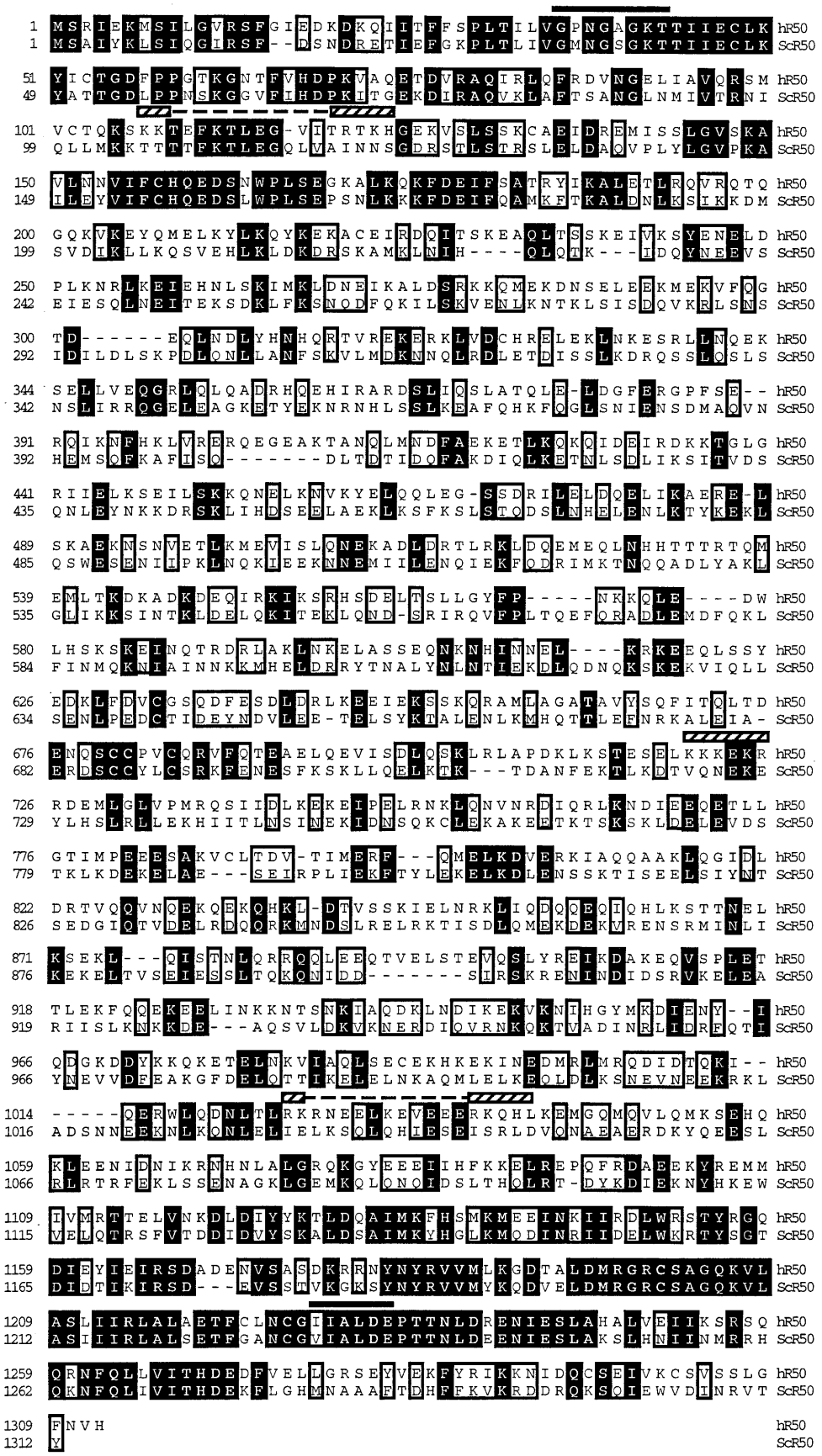

FIG. 2. Alignment of hRad50 and ScRad50. Identical residues are shaded, and similarities are boxed. The following amino acids were considered similar: D, E, N, and Q; F, W, and Y; K and R; A and G; I and V; L and M; S and T; C; H; and P. Potential nuclear localization signals are indicated by hatched boxes over the hRad50 sequence. Two of these are bipartite (67); a dashed line connects the two segments. The Walker A and B NTP binding domains are overlined.

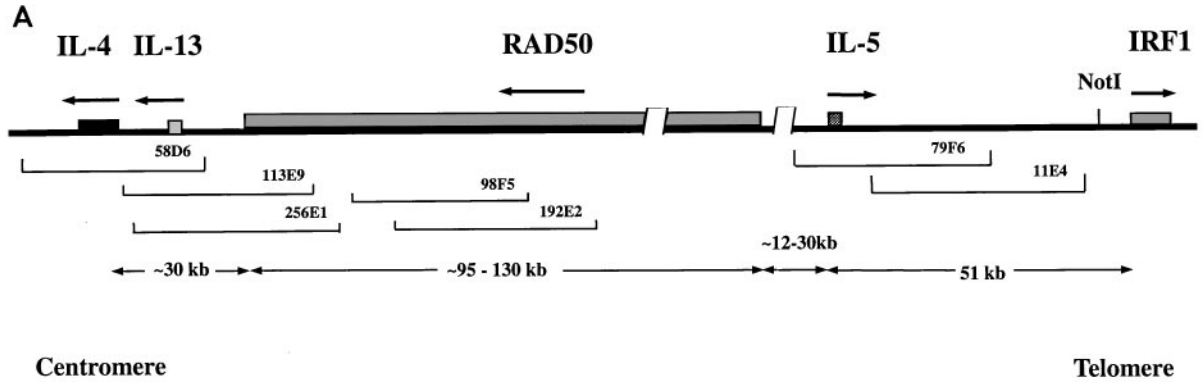

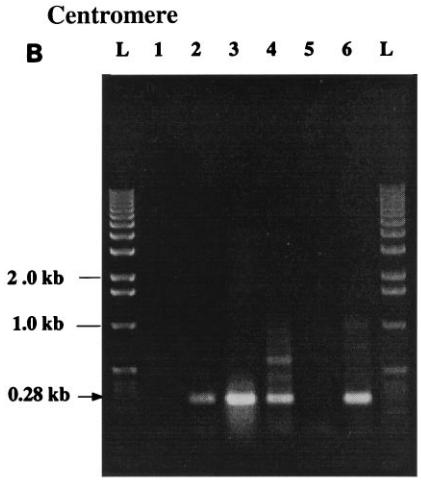

FIG. 3. Chromosomal localization of the *hRAD50* locus. (A) Physical mapping of the human *RAD50* gene within the cytokine gene cluster in the 5q23-q31 interval. The genes depicted at the top map to a 320-kb *Not*I restriction fragment at 5q31. The distance between the *IL4* and *IL5* genes is 150 to 200 kb. Because of the gaps in the chromosome 5-specific cosmid contig, represented by a double broken line, accurate estimation of the distance between the *RAD50* and the *IL5* genes, as well as of the size of the genomic *RAD50*, was not feasible. Some of the *hRAD50* cosmid clones described in the text are depicted below the map. Directions of gene transcription are indicated by the arrows. The detailed physical mapping of this region will be published elsewhere (16a) along with the transcriptional mapping of the 1.2-Mb cytokine gene cluster region in the 5q23-q31 interval. (B) PCR using primers G10-2 and G10-14 (see Materials and Methods and Table 1), based on the 5′ untranslated region of *hRAD50*, was carried out to confirm the location of the *hRAD50* locus. Template DNAs were as follows: lane 1, no-DNA control; lane 2, human genomic DNA; lane 3, YAC 854G6; lane 4, HHW105 human-hamster hybrid; lane 5, CHO genomic DNA; lane 6, YAC A94G6. Lane L, 1-kb ladder.

failed to give any product (Fig. 3B). Four additional cosmid clones, 54A2, 98F5, 192E2, and 32H4, were obtained by further screening of the chromosome 5-specific cosmid library with additional *hRAD50* cDNA segments. By mapping various portions of the *hRAD50* coding sequence to *hRAD50*-containing cosmids and YAC clones, we determined that the *hRAD50* gene spans 100 to 130 kb (Fig. 3A). Because of the gaps in the existing cosmid contig, it was not possible to determine the size of the gene more precisely.

DNA sequence analysis of *hRAD50*. *hRAD50* is highly conserved at the N and C termini, exhibiting greater than 50% identity in these regions (Fig. 2 and 4A). A second apparent *ScRAD50* homolog has been identified among randomly sequenced *Caenorhabditis elegans* cDNAs and is similarly conserved at the N terminus (cDNA clone D37392 [38a]). hRad50 contains three potential nuclear localization signals (Fig. 2), consistent with immunofluorescence analysis that demonstrates that hRad50 is a nuclear protein (53a). The conserved N-terminal domain includes the Walker A-type ATP binding signature (3, 24), whereas the Walker B-type DA box is encoded by the C-terminal conserved region (24, 30). The DA box-containing region of hRad50 is the most conserved region of the protein, exhibiting 68% identity over the C-terminal 270 amino acids (Fig. 2 and 4A). The internal portion of ScRad50 is conserved to a much lesser extent. This region encodes the heptad repeat regions of the protein from amino acids 177 to 421 and amino acids 743 to 995 (3). Although the functional relevance of the heptad repeat motif in ScRad50 is not well established, it is likely to be significant for the assembly of ScRad50-containing protein complexes (3, 66). We used the COILS program, which calculates the probability that a given segment of a protein will adopt a coiled-coil conformation, to compare the predicted secondary structures of the two Rad50 homologs (52). The extent of similarity and identity between the two Rad50 proteins was determined over consecutive, nonoverlapping 130-amino-acid segments (Fig. 4A) and is plotted in comparison with the probabilities determined by the COILS program (52) (Fig. 4B). In spite of the relatively divergent primary sequence of the heptad repeat domains, these regions in hRad50 and ScRad50 are predicted to adopt extremely similar coiled-coil structures.

***hRAD50* expression.** *hRAD50* expression was assessed by Northern blotting of mRNA prepared from various human tissues, using the A1 cDNA (Fig. 1) as a probe. The 5.5-kb *hRAD50* transcript is seen in the testis but is barely detectable in the other tissues examined (Fig. 5A). A faintly hybridizing band is also seen at 7 kb. The origin of this signal has not been established. Since a single protein species is observed with hRad50 antiserum (Fig. 5B), the 7-kb band most likely corresponds to alternative 3′-end processing of the *hRAD50* transcript. Support for this explanation comes from the structure of the A106 cDNA, which contains evidence of alternative 3′-end processing (Fig. 1) (16). Increased expression of *hRAD50* in the testis is reminiscent of the *hMRE11* expression pattern as well as that of another mammalian *RAD52* epistasis group member, *RAD51* (65, 75). We have also detected *hRAD50* transcripts in fetal liver and in activated T and B cells by reverse transcriptase PCR (data not shown). As shown by Western blotting and immunoprecipitation (see below), the hRad50 protein is readily detectable in normal fibroblasts and established lymphoid cell lines, where the level of mRNA is three- to fivefold lower than that observed in the testis (data not shown and Fig. 5B and 6). The fact that we readily detect hRad50 protein in cell lines which do not contain high steady-

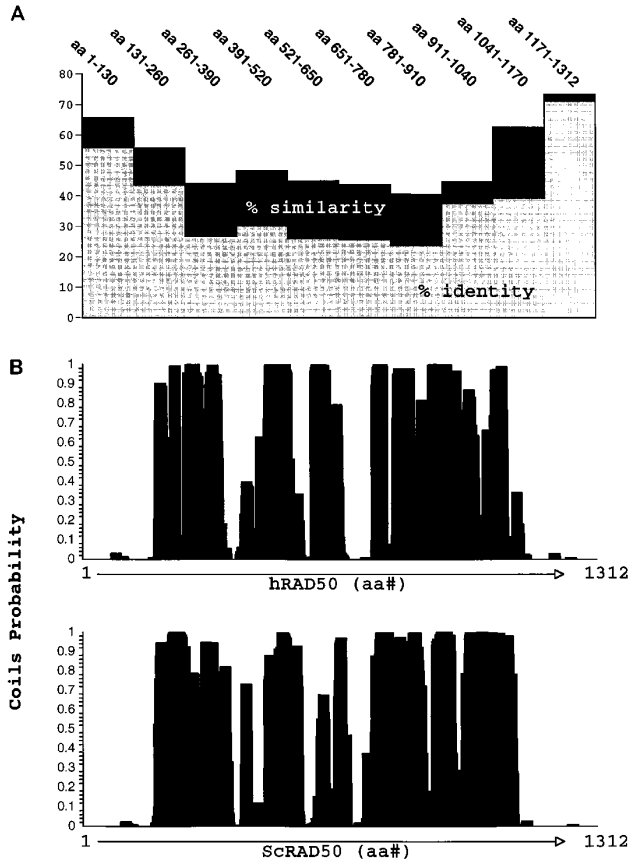

FIG. 4. Pairwise comparison of Rad50 homologs. (A) hRad50 and ScRad50 were compared pairwise in 130-amino-acid (aa) segments, using the Lipman-Pearson algorithm (49) with residues weighted according to the PAM250 matrix (13) (shaded in black) or scored by identity only (unshaded). (B) hRad50 and ScRad50 were analyzed by using the COILS program (52). Shown are the data at window width 28 (without weighting of positions a and d). The COILS program was accessed on the World Wide Web at http://ulrec3.unil.ch/software/COILS_form.html. Numerical output was downloaded into Deltagraph Pro (Delta Point, Monterey, Calif.) for creation of the graph shown.

state levels of hRAD50 mRNA suggests that the protein is relatively long lived.

Given its presumptive role in the repair of IR-induced DNA damage, we tested whether the expression of *hRAD50* was modulated in response to IR. Logarithmically growing primary diploid fibroblasts (IMR90) were irradiated, and whole-cell extracts were analyzed by Western blot analysis with an hRad50 polyclonal antiserum. The steady-state level of hRad50 protein does not change in response to IR (Fig. 5B). We have also observed constitutive (i.e., noninducible) expression of hMre11. However, the subnuclear distribution of the hMre11 protein is specifically altered by IR. We are currently examining whether hRad50 exhibits similar behavior (53a).

hRad50 protein complexes. Recently, Johzhuka and Ogawa reported that scMre11 interacts with both ScRad50 and ScXrs2 in a two-hybrid system (36). We tested whether an analogous complex involving hMre11 and hRad50 exists in human cells. hMre11 antiserum or hRad50 antiserum was used for immunoprecipitation from whole-cell extracts of the human lymphoblastoid cell line TK6 (48). Since we observe nuclear staining with hMre11 and hRad50 antisera (data not shown), we prepared whole-cell extracts in high salt (500 mM NaCl) to increase the yield of chromatin-associated nuclear proteins (9). These extracts were diluted to 300 mM NaCl for immunoprecipitation as described in Materials and Methods. Immunoprecipitated material was analyzed by immunoblotting with hRad50 antiserum or hMre11 antiserum (Fig. 6A). Filters were then stripped and retreated with the converse antiserum, αhMre11 (following αhRad50) or αhRad50 (following αhMre11). A single 153-kDa band, corresponding to the predicted size of the hRad50 protein, is precipitated by the hRad50 antiserum but not by the preimmune serum (Fig. 6A, lanes 5 and 6). The hRad50 antiserum also recognizes an identical 153-kDa band in the material immunoprecipitated by the hMre11 antiserum (Fig. 6A, lane 4). Conversely, a single 81-kDa band corresponding to the hMre11 protein is precipitated by the hMre11 antiserum as well as the hRad50 antiserum (Fig. 6A, lanes 2 and 7). Immunoblotting the precipitated material with preimmune serum produces neither the 81-kDa nor the 153 kDa signal observed with the specific antisera (data not shown).

Association of these proteins in 300 mM NaCl demonstrates that hRad50 and hMre11 are in stable association. To assess the stability of this complex in more detail, immunoprecipitations were carried out at NaCl concentrations ranging from 300 to 1,000 mM, followed by immunoblotting with hMre11 and hRad50 antisera as described above (Fig. 6B). The amount

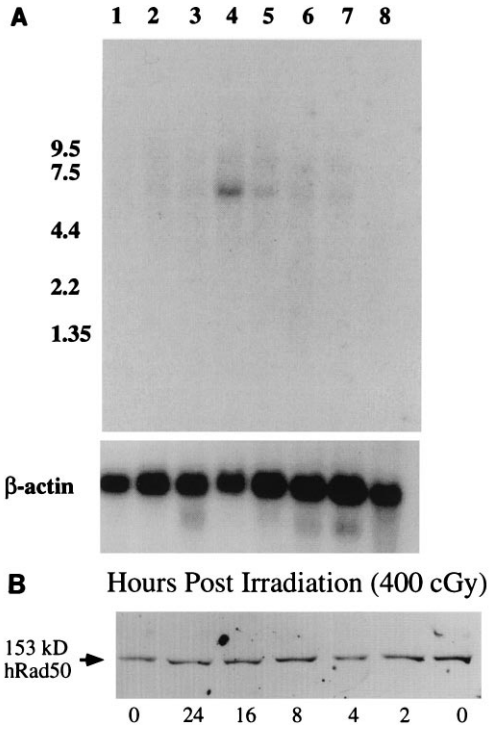

FIG. 5. *hRAD50* expression. (A) A Northern blot filter was prepared with 1.5 μg of poly(A)$^+$ RNA from various human tissues (Clontech). Hybridization with a probe derived from the full-length *hRAD50* cDNA was carried out as described in Materials and Methods. The positions of RNA size standards are indicated in kilobases. β-Actin hybridization was included to control for mRNA abundance. Lanes: 1, spleen; 2, thymus; 3, prostate; 4, testis; 5, ovary; 6, small intestine; 7, colon; 8, peripheral blood leukocytes. (B) Logarithmically growing IMR90 fibroblasts (6×10^5 cells per lane) were irradiated at a dose of 400 cGy, harvested at the indicated times following irradiation, and processed for immunoblot analysis as described in Materials and Methods. Cell lysates were fractionated by SDS-PAGE on 7.0% gels before transfer to nitrocellulose filters. hRad50 antiserum was diluted 1:400, and bound antibody was detected with horseradish peroxidase-conjugated protein G plus protein A. Detection was effected by chemiluminescence, using the Luminol reagent (Pierce). Required exposure times varied from 10 to 45 s.

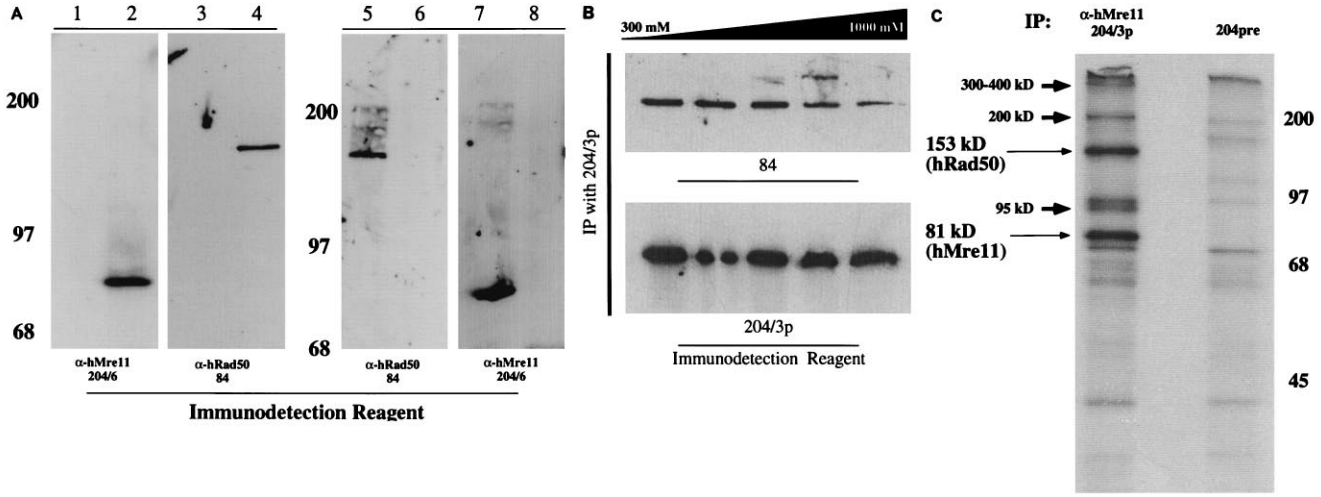

FIG. 6. Immunoprecipitation analyses. (A) TK6 cells (2.5×10^6 per lane) were lysed in high-salt buffer (see Materials and Methods) and diluted 1:2 in standard lysis buffer. Following incubation with the indicated antisera, immunoprecipitation was carried out with protein A-Sepharose beads and immunoprecipitated material was analyzed by immunoblotting. The positions of protein molecular mass standards are indicated in kilodaltons. Filters were then stripped and retreated. Lane pairs 1-2 and 3-4 represent the same filter; lane pairs 5-6 and 7-8 represent the same filter. Immunoprecipitation with 204pre (lanes 1 and 3) or αhMre11 204/6 (lanes 2 and 4) was followed by immunodetection with αhMre11 204/6 (lanes 1 and 2) or αhRad50 84 (lanes 3 and 4). Immunoprecipitation with 84pre (lanes 6 and 8) or αhRad50 84 (lanes 5 and 7) was followed by immunodetection with αhRad50 84 (lanes 5 and 6) or αhMre11 204/6 (lanes 7 and 8). (B) K562 cells (2.5×10^6 per lane) were lysed in high-salt buffer as described above and diluted 1:2 in lysis buffer with increasing NaCl. Following incubation with 204/3p antiserum (affinity-purified αhMre11), immunoprecipitation was carried out with protein A-Sepharose beads and immunoprecipitated material was analyzed by immunoblotting with 204/3p. Filters were then stripped and retreated with serum 84 (αhRad50). From left to right, NaCl concentrations were 300, 500, 750, 850, and 1,000 mM. (C) K562 cells (5×10^6 per lane) were grown in the presence of [^{35}S]methionine for 6 h and lysed in high-salt buffer. Immunoprecipitation was carried out as described in Materials and Methods, using 204/3p (affinity-purified αhMre11) or 204pre antiserum. Immunoprecipitated material was analyzed by SDS-PAGE on 8.5% gels. The gels were then dried and autoradiographed for 13 h. The positions of protein molecular mass standards are indicated at the right.

of hMre11 protein immunoprecipitated at increasing salt concentrations is unchanged. Similarly, the relative abundance of coimmunoprecipitated hRad50 remains essentially constant until the NaCl concentration exceeds 750 mM, and it is still detectable at 1,000 mM NaCl (Fig. 6B). These data demonstrate that the hRad50-hMre11 association is highly stable. Further analyses are required to assess the relative affinity of this interaction.

In *S. cerevisiae*, ScMre11 is associated with ScRad50 as well as with the 96-kDa protein, ScXrs2 (36). Having demonstrated the association of hRad50 and hMre11, we carried out immunoprecipitation experiments from metabolically labeled cells to determine whether the hRad50-hMre11 complex was associated with a protein corresponding to hXrs2. Cells were labeled continuously for 6 h with [^{35}S]methionine and lysed in high-salt buffer as described above before immunoprecipitation with 204/3p (affinity-purified αhMre11) or 204pre (preimmune serum). Following fractionation by SDS-polyacrylamide gel electrophoresis (PAGE), immunoprecipitated material was visualized by autoradiography (Fig. 6C). As expected, bands of 81 and 153 kDa corresponding to hMre11 and hRad50 were immunoprecipitated by the hMre11 antiserum. However, three additional bands of 95 and 200 kDa and a species at approximately 350 kDa also are present among the immunoprecipitated material. These three proteins are not present in the control immunoprecipitation reaction (Fig. 6C), suggesting that hRad50 and three proteins of 95, 200, and 350 kDa physically associate with hMre11. The detection of a 95-kDa species among the immunoprecipitated material further suggests that the human hRad50-hMre11 complex contains the human Xrs2 homolog. Confirmation of this hypothesis requires antiserum that recognizes the presumptive hXrs2 protein.

DISCUSSION

Isolation of the human *RAD50* homolog. We undertook the isolation of genes contained in the 5q23-q31 chromosomal interval because of the strong correlation between AML and chromosomal aberrations involving this region. In this report, we show that a human *RAD50* homolog, *hRAD50*, is situated at the chromosomal region 5q31.1, the region most commonly deleted in AML. We demonstrate that the hRad50 protein exists in a stable complex with hMre11, as has been shown for the *S. cerevisiae* homologs (36). Thus, the multiprotein complexes in which these DSB repair proteins function are conserved. Maximal expression of *hRAD50* is confined to the testes, suggesting that, like its yeast counterpart, this protein plays a role in meiotic recombination (3). Similar observations have been made for the human *RAD51* and *MRE11* homologs (65, 73).

Except for the N- and C-terminal domains, where the Rad50 homologs are extremely similar, *hRAD50* is somewhat less conserved than other mammalian *RAD52* epistasis group members identified to date (5, 65, 75). However, the predicted hRad50 protein does retain the structural motifs of the yeast homolog. Walker A- and B-type NTP binding domains are predicted at the N and C termini of both Rad50 homologs, and these domains are more than 50% identical between yeast and human sequences (Fig. 2 and 4A). The coiled-coil domain structure of ScRad50 (3) is also predicted to exist in hRad50, despite a rather modest level of primary sequence conservation over the corresponding regions of the protein (Fig. 4). On the basis of the coiled-coil domains of ScRad50 and physical properties of the purified protein, it has been suggested that ScRad50 exists as a homodimer (66). Thus far, we have been unable to demonstrate self-association of hRad50, using a two-hybrid system in *S. cerevisiae.*

Similarity in the structures of hRad50/ScRad50 and members of the SMC gene family may offer some insight into their biochemical functions (24, 30, 69). Of particular interest is the similarity between hRad50, ScRad50, and the *Escherichia coli* protein SbcC (30, 69). The Rad50 and SbcC proteins contain analogous structural domains; the three proteins contain Walker A and B NTP binding domains at the N and C termini separated by a heptad repeat-containing region in which modest sequence similarity is observed (30). SbcC functions in complex with a coordinately regulated protein, SbcD, to mediate ATP-dependent exonuclease activity (12a, 40). It is interesting that the three known Mre11 homologs exhibit significant homology to the SbcD proteins from *E. coli* and *Bacillus subtilis* (23, 39, 43). Similarity between SbcC/SbcD and ScRad50/ScMre11 has been noted previously (72). In light of our demonstration here that hRad50 exists in a stable complex with hMre11, we hypothesize that the hRad50-hMre11 complex is a mammalian analog of the SbcC/SbcD exonuclease. Consistent with this hypothesis is the indication that the rate of 5′-to-3′ exonucleolytic strand processing during DSB repair is reduced in *Scrad50* mutants (32, 33). However, it is not clear how loss of this putative exonucleolytic function could account for the increased rate of spontaneous mitotic recombination in *Scrad50* or *Scmre11* mutants (1, 2). Our hypothesis would thus require that the hRad50-hMre11 complex is also involved in other aspects of the recombination reaction.

Immunoprecipitation from metabolically labeled cells suggests that hMre11 and hRad50 associate with three other proteins. Of particular interest is the presence of a 95-kDa protein in the immunoprecipitated material. Since the size of this protein is in excellent agreement with the predicted molecular mass of ScXrs2 (31), we speculate that this 95-kDa band corresponds to the human Xrs2 homolog. We are hopeful that our ability to immunoprecipitate this putative human Xrs2 homolog will provide a means to isolate the *hXRS2* gene. The identities of the 200- and 350-kDa proteins associated with hRad50 and hMre11 are unclear. Biochemical characterization of these additional components is required in order to fully elucidate the composition and function of hRad50-hMre11-containing protein complexes.

Why is the mammalian *RAD52* epistasis group conserved? Recombinational DNA repair can proceed by homology-dependent or independent (i.e., illegitimate) mechanisms. Both modes of recombination are observed in *S. cerevisiae* as well as mammals (41, 56, 64, 68, 83). In yeast cells, homology-dependent repair involving sister chromatids predominates over illegitimate recombination (38, 41, 56), whereas in mammalian cells, DSB repair by illegitimate recombination is highly favored (68). The strong preference for homologous recombination between sister chromatids in yeast cells is likely to account for the observation that cells in G_1, during which sister chromatids are absent, are more sensitive to IR-induced double strand breaks than cells in G_2 (20). In mammalian cells, disproportionate G_1 sensitivity to IR is not seen in wild-type cells but is observed in the Chinese hamster cell mutant XR-1 (77). The G_1 sensitivity of XR-1 has been explicitly attributed to a G_1-specific defect in DSB repair (22). The phenotype of XR-1 suggests that two mammalian DSB repair pathways which differ in their dependence on sister chromatids may exist in mammalian cells. The conservation of mammalian *RAD52* epistasis group homologs (5, 65, 75) strongly implies that one of these is analogous to the yeast DSB repair pathway. In light of the dependence on sister chromatids observed in *S. cerevisiae*, it is logical to conclude that the mammalian *RAD52* epistasis group is analogously relevant for DSB repair following DNA replication. Since the *xrcc4* mutant cell exhibits G_1-specific IR sensitivity and given the fact that *XRCC4* is unrelated to members of the *RAD52* epistasis group (7), this gene represents the complementary mammalian pathway that effects DSB repair in G_1. In the absence of the pathway represented by *XRCC4*, mammalian DSB repair thus behaves more like that seen in *S. cerevisiae*. Therefore, it will be of considerable interest to assess whether mammalian *RAD52* epistasis group mutants exhibit differential sensitivity to IR and DSB repair deficiency in G_2. Targeted mutation of the *RAD50* locus will contribute to the resolution of this issue.

Recombinational repair deficiency and tumorigenesis. We have mapped the *hRAD50* locus to 5q31. Deletions and other rearrangements at 5q31 are frequently associated with AML and preleukemic myelodysplasia (25, 44, 45, 63). Alterations that include 5q31 are also seen in therapy-related malignancies (14, 61). This chromosomal region is thus of central importance in determining the onset of myeloid leukemia, and the placement of the *hRAD50* locus at 5q31 suggests that this gene be considered a potential AML tumor suppressor (44). Chromosome loss and rearrangement are very common somatically acquired genetic alterations in malignant cells. Yeast *rad50*, *mre11*, and *xrs2* mutants are associated with an increased rate of homologous recombination (1, 2, 33) and a dramatically elevated rate of spontaneous chromosome loss (80). It is likely that a similar phenotypic outcome in human cells would potentiate the process of tumorigenesis. Hence, in addition to the chromosomal location of *hRAD50*, a potential role for *RAD50*, *MRE11*, or *XRS2* mutations in tumorigenesis is also suggested by the corresponding yeast phenotypes. Interestingly, cell lines representing the chromosomal instability syndromes Bloom syndrome and ataxia telangiectasia exhibit similar features (10, 42, 55), and both are associated with high rates of malignancy (12, 21, 62). In this regard, it is intriguing that the *hMRE11* locus also maps to a chromosomal region associated with malignancy, 11q21 (65). The importance of increased recombination rates in malignancy is further suggested by DNA mismatch repair-deficient mice (*msh2* knockout mice), which are predisposed to cancer (15). We are currently investigating the structure of the *hRAD50* locus in 5q31-altered patient material to ascertain whether mutations in the *hRAD50* gene are correlated with the 5q31-associated myeloid malignancy.

ACKNOWLEDGMENTS

This work was supported by ACS grant NP-918 (J.H.J.P.) and an ACS IRG grant 35-36-5 (J.H.J.P.). J.H.J.P. is a Special Fellow of the Leukemia Society of America. This work was supported in part from a grant to the University of Wisconsin Medical School under the Howard Hughes Medical Institute Research Resources Program for Medical Schools. D.A.B. and R.S.M. are supported by NIH predoctoral training grant 5T32GM07133.

We thank Kirsten J. Monsen for expert technical assistance, Mary Ellen Perry and Robert DeMars for advice on immunological methods, members of the Barton, Anderson, and Culbertson laboratories at the University of Wisconsin for assistance and materials, Bill Engels for graphics assistance, and Eugene Koonin and Mark P. Krebs for helpful discussions. We also thank Mary Ellen Perry, Kathy Barton, Carlos Flores, and Allen Laughon for critical review of the manuscript.

REFERENCES

1. **Ajimura, M., S.-H. Leem, and H. Ogawa.** 1993. Identification of new genes required for meiotic recombination in *Saccharomyces cerevisiae*. Genetics **133:**51–66.
2. **Alani, E., R. Padmore, and N. Kleckner.** 1990. Analysis of wild-type and *rad50* mutants of yeast suggests an intimate relationship between meiotic chromosome synapsis and recombination. Cell **61:**419–436.
3. **Alani, E., S. Subbiah, and N. Kleckner.** 1989. The yeast *RAD50* gene encodes a predicted 153 kD protein containing a purine nucleotide-binding domain and two large heptad repeat regions. Genetics **122:**47–57.
4. **Ausubel, F. M., R. Brent, R. E. Kingston, D. D. Moore, J. G. Seidman, J. A.**

Smith, and K. Struhl (ed.). 1989. Current protocols in molecular biology, vol. 1–3. John Wiley & Sons, New York.
5. **Bendixen, C., I. Sunjevaric, R. Bauchwitz, and R. Rothstein.** 1994. Identification of a mouse homologue of the *Saccharomyces cerevisiae* recombination and repair gene, *RAD52*. Genomics **23:**300–303.
6. **Biedermann, K. A., J. Sun, A. J. Giaccia, L. M. Tosto, and J. M. Brown.** 1991. scid mutation in mice confers hypersensitivity to ionizing radiation and a deficiency in DNA double-strand break repair. Proc. Natl. Acad. Sci. USA **88:**1394–1397.
7. **Blunt, T., N. J. Finnie, G. E. Taccioli, G. C. Smith, J. Demengeot, T. M. Gottlieb, R. Mizuta, A. J. Varghese, F. W. Alt, P. A. Jeggo, and S. P. Jackson.** 1995. Defective DNA-dependent protein kinase activity is linked to V(D)J recombination and DNA repair defects associated with the murine scid mutation. Cell **80:**813–823.
8. **Bollag, R. J., A. S. Waldman, and R. M. Liskay.** 1989. Homologous recombination in mammalian cells. Annu. Rev. Genet. **23:**199–225.
9. **Boubnov, N. V., K. T. Hall, Z. Wills, S. E. Lee, D. M. He, D. M. Benjamin, C. R. Pulaski, H. Band, W. Reeves, E. A. Hendrickson, and D. T. Weaver.** 1995. Complementation of the ionizing radiation sensitivity, DNA end binding, and V(D)J recombination defects of double-strand break repair mutants by the p86 Ku autoantigen. Proc. Natl. Acad. Sci. USA **92:**890–894.
10. **Chaganti, R. S. K., S. Schonberg, and J. A. German.** 1974. A many fold increase in sister chromatid exchange in Bloom's syndrome lymphocytes. Proc. Natl. Acad. Sci. USA **71:**4508–4512.
11. **Chumakov, I., P. Rigault, S. Guillow, P. Ougen, A. Aillaut, G. Guasconi, P. Gervy, I. Legall, P. Soularue, L. Grinas, L. Bougueleret, C. Bellanne-Chantelot, B. Lacroix, E. Barillot, P. Gesnouin, S. Pook, G. Vaysseix, G. Frelat, A. Schmitz, J.-L. Sambucy, A. Bosch, X. Estivill, J. Weissenbach, A. Vignal, H. Riethman, D. Cox, D. Patterson, K. Gardiner, M. Hattori, Y. Sakaki, H. Ichikawa, M. Ohki, Le Paslier, D., R. Heilig, S. Antonarakis, and D. Cohen.** 1992. Continuum of overlapping clones spanning the entire human chromosome 21q. Nature (London) **359:**380–387.
12. **Cleaver, J. E.** 1989. DNA repair in man. Birth Defects **25:**61–82.
12a. **Connelly, J., and D. R. Leach.** Unpublished data.
13. **Dayhoff, M. O. (ed.).** 1978. A model of evolutionary change in proteins. Matrices for detecting distant relationships, supplement, 3rd ed., vol. 5. National Biomedical Research Foundation, Washington, D.C.
14. **Devereux, S.** 1991. Therapy associated leukaemia. Blood Rev. **5:**138–145.
15. **de Wind, N., M. Dekker, A. Berns, M. Radman, and H. te Riele.** 1995. Inactivation of the mouse *Msh2* gene results in mismatch repair deficiency, methylation tolerance, hyperrecombination, and predisposition to cancer. Cell **82:**321–330.
16. **Dolganov, G. M.** Unpublished data.
16a. **Dolganov, G. M., et al.** Unpublished data.
17. **Donovan, J. W., G. T. Milne, and D. T. Weaver.** 1994. Homotypic and heterotypic protein associations control RAD51 function in double strand break repair. Genes Dev. **8:**2552–2562.
18. **Feinberg, A. P., and B. Vogelstein.** 1983. A technique for radiolabeling DNA restriction endonuclease fragments to high specific activity. Anal. Biochem. **132:**6–13.
19. **Fischer, S. G., E. Cayanis, M. D. F. Bonaldo, A. M. Bowcock, L. L. Deaven, I. S. Edelman, T. Gallardo, S. Kalachikov, L. Lawton, J. L. Longmire, M. Lovett, S. Osborne-Lawrence, R. Rothstein, J. J. Russo, M. B. Soares, I. Sunjevaric, V. S. Venkatraj, D. Warburton, P. Zhang, and A. Efstratiadis.** 1996. A high-resolution annotated physical map of the human chromosome 13q12-13 region containing the breast cancer susceptibility locus *BRCA2*. Proc. Natl. Acad. Sci. USA **93:**690–694.
20. **Game, J. C.** 1993. DNA double strand breaks and the *RAD50-RAD57* genes in *Saccharomyces*. Cancer Biol. **4:**73–83.
21. **German, J.** 1983. Patterns of neoplasia associated with the chromosome-breakage syndromes, p. 11–21. *In* J. German (ed.), Chromosome mutation & neoplasia. Alan R. Liss, New York.
22. **Giaccia, A., R. Weinstein, J. Hu, and T. D. Stamato.** 1985. Cell cycle-dependent repair of double-strand DNA breaks in a gamma-ray-sensitive Chinese hamster cell. Somatic Cell Mol. Genet. **11:**485–491.
23. **Gibson, F. P., D. R. F. Leach, and R. G. Lloyd.** 1992. Identification of *sbcD* mutations as cosuppressors of *recBC* that allow propogation of DNA palindromes in *Escherichia coli* K-12. J. Bacteriol. **174:**1222–1228.
24. **Gorbalenya, A. E., and E. V. Koonin.** 1990. Superfamily of UvrA-related NTP-binding proteins. Implications for rational classification of recombination/repair systems. J. Mol. Biol. **213:**583–591.
25. **Groupe Français de Cytogénétique Hématologique.** 1993. Collaborative study of karyotypes in childhood acute lymphoblastic leukemias. Leukemia **7:**10–1926.
26. **Haber, J. E.** 1992. Exploring the pathways of homologous recombination. Curr. Opin. Cell Biol. **4:**401–412.
27. **Harlow, E., and D. Lane.** 1988. Antibodies: a laboratory manual. Cold Spring Harbor Laboratory, Cold Spring Harbor, N.Y.
28. **Hays, S. L., A. A. Firmenich, and P. Berg.** 1995. Complex formation in yeast double-strand break repair: participation of Rad51, Rad52, Rad55, and Rad57 proteins. Proc. Natl. Acad. Sci. USA **92:**6925–6929.
29. **Hendrickson, E. A., X.-Q. Qin, E. A. Bump, D. G. Schatz, M. Oettinger, and D. T. Weaver.** 1991. A link between double-strand break-related repair and V(D)J recombination: the scid mutation. Proc. Natl. Acad. Sci. USA **88:** 4061–4065.
30. **Hirano, T., T. J. Mitchison, and J. R. Swedlow.** 1995. The SMC family: from chromosome condensation to dosage compensation. Curr. Opin. Cell Biol. **7:**329–336.
31. **Ivanov, E. L., V. G. Korolev, and F. Fabre.** 1992. *XRS2*, a DNA repair gene of *Saccharomyces cerevisiae*, is needed for meiotic recombination. Genetics **132:**651–664.
32. **Ivanov, E. L., N. Sugawara, J. Fishman-Lobell, and J. E. Haber.** 1996. Genetic requirements for the single-strand annealing pathway of double-strand break repair in *Saccharomyces cerevisiae*. Genetics **142:**693–704.
33. **Ivanov, E. L., N. Sugawara, C. I. White, F. Fabre, and J. E. Haber.** 1994. Mutations in *XRS2* and *RAD50* delay but do not prevent mating-type switching in *Saccharomyces cerevisiae*. Mol. Cell. Biol. **14:**3414–3425.
34. **Jeggo, P. A., and L. M. Kemp.** 1983. X-ray sensitive mutants of Chinese hamster ovary cell line: isolation and cross-sensitivity to other DNA damaging agents. Mutat. Res. **112:**313–327.
35. **Jeggo, P. A., J. Tesmer, and D. J. Chen.** 1991. Genetic analysis of ionising radiation sensitive mutants of cultured mammalian cell lines. Mutat. Res. **254:**125–133.
36. **Johzhuka, K., and H. Ogawa.** 1995. Interaction of Mre11 and Rad50: two proteins required for DNA repair and meiosis-specific double-strand break formation in *Saccharomyces cerevisiae*. Genetics **139:**1521–1532.
37. **Jones, N. J., R. Cox, and J. Thacker.** 1988. Six complementation groups for ionising radiation sensitivity in Chinese hamster cells. Mutat. Res. **193:**139–144.
38. **Kadyk, L. C., and L. H. Hartwell.** 1992. Sister chromatids are preferred over homologs as substrates for recombinational repair in *Saccharomyces cerevisiae*. Genetics **132:**387–402.
38a. **Kohara, Y.** Unpublished data.
39. **Koonin, E. V.** 1994. Conserved sequence pattern in a wide variety of phosphoesterases. Protein Sci. **3:**356–358.
40. **Kowalczykowski, S. C., D. A. Dixon, A. K. Eggleston, S. D. Lauder, and W. M. Rehrauer.** 1994. Biochemistry of homologous recombination in *Escherichia coli*. Microbiol. Rev. **58:**401–465.
41. **Kramer, K. M., J. A. Brock, K. Bloom, J. K. Moore, and J. E. Haber.** 1994. Two different types of double-strand breaks in *Saccharomyces cerevisiae* are repaired by similar *RAD52*-independent, nonhomologous recombination events. Mol. Cell. Biol. **14:**1293–1301.
42. **Langlois, R. G., W. L. Bigbee, R. H. Jensen, and J. German.** 1989. Evidence for increased in vivo mutation and somatic recombination in Bloom's syndrome. Proc. Natl. Acad. Sci. USA **86:**670–674.
43. **Leach, D. R. F., R. G. Lloyd, and A. F. W. Coulson.** 1992. The SbcCD protein of Escherichia coli is related to two putative nucleases in the UvrA superfamily of nucleotide-binding proteins. Genetica **87:**95–100.
44. **Le Beau, M.** 1992. Deletions of chromosome 5 in malignant myeloid disorders. Cancer Surv. **15:**143–159.
45. **Le Beau, M., R. Espinosa, W. L. Neuman, W. Stock, D. Roulston, R. A. Larson, M. Keinanen, and C. A. Westbrook.** 1993. Cytogenetic and molecular delineation of the smallest commonly deleted region of chromosome 5 in malignant myeloid diseases. Proc. Natl. Acad. Sci. USA **90:**5484–5488.
46. **Le Beau, M. M., K. S. Albain, R. A. Larson, J. W. Vardiman, E. M. Davis, R. R. Blough, H. M. Golomb, and J. D. Rowley.** 1986. Clinical and cytogenetic correlations in 63 patients with therapy-related myelodysplastic syndromes and acute nonlymphocytic leukemia: further evidence for characteristic abnormalities of chromosomes no. 5 and 7. J. Clin. Oncol. **4:**325–345.
47. **Lee, S. E., C. R. Pulaski, D. M. He, D. M. Benjamin, M. Voss, J. Um, and E. A. Hendrickson.** 1995. Isolation of mammalian cell mutants that are X-ray sensitive, impaired in DNA double-strand break repair and defective for V(D)J recombination. Mutat. Res. **336:**279–291.
48. **Liber, H. L., and W. G. Thilly.** 1982. Mutation assay at the thymidine kinase locus in diploid human lymphoblasts. Mutat. Res. **94:**467–485.
49. **Lipman, D. J., and W. R. Pearson.** 1985. Rapid and sensitive protein similarity searches. Science **227:**1435–1441.
50. **Longmire, J. L., N. C. Brown, L. J. Meincke, M. L. Campbell, K. L. Albright, J. J. Fawcett, E. W. Campbell, R. K. Moyzis, C. E. Hildebrand, G. A. Evans, and L. L. Deavon.** 1993. Construction and characterization of partial digest DNA libraries made from flow-sorted human chromosome 16. Genet. Anal. Tech. Appl. **10:**69–76.
51. **Lovett, M., J. Kere, and L. M. Hinton.** 1991. Direct selection: a method for the isolation of cDNAs encoded by large genomic regions. Proc. Natl. Acad. Sci. USA **88:**9628–9632.
52. **Lupas, A., M. Van Dyke, and J. Stock.** 1991. Predicting coiled coils from protein sequences. Science **252:**1162–1164.
53. **Malone, R. E., T. Ward, S. Lin, and J. Waring.** 1990. The *RAD50* gene, a member of the double strand break repair epistasis group, is not required for spontaneous mitotic recombination in yeast. Curr. Genet. **18:**111–116.
53a. **Maser, R. S., K. J. Monsen, and J. H. J. Petrini.** Unpublished data.
54. **McLachlan, A., and J. Karn.** 1982. Periodic charge distributions in the myosin rod amino acid sequence match cross-bridge spacings in muscle. Nature (London) **299:**226–231.

55. **Meyn, M. S.** 1993. High spontaneous rates of intrachromosomal recombination in ataxia-telangiectasia. Science **260:**1327–1330.
56. **Mezard, C., and A. Nicolas.** 1994. Homologous, homeologous, and illegitimate repair of double-strand breaks during transformation of a wild-type strain and a *rad52* mutant strain of *Saccharomyces cerevisiae*. Mol. Cell. Biol. **14:**1278–1292.
57. **Milne, G. T., and D. T. Weaver.** 1993. Dominant negative alleles of *RAD52* reveal a DNA repair/recombination complex including Rad51 and Rad52. Genes Dev. **7:**1755–1765.
58. **Moore, J. K., and J. E. Haber.** 1996. Cell cycle and genetic requirements of two pathways of nonhomologous end-joining repair of double-strand breaks in *Saccharomyces cerevisiae*. Mol. Cell. Biol. **16:**2164–2173.
59. **Morgan, J. G., G. M. Dolganov, S. E. Robbins, L. M. Hinton, and M. Lovett.** 1992. The selective isolation of novel cDNAs encoded by the regions surrounding the human interleukin 4 and 5 genes. Nucleic Acids Res. **20:**5173–5179.
60. **Nagarajan, L., J. Zavadil, D. Claxton, X. Lu, J. Fairman, J. A. Warrington, J. J. Wasmuth, A. C. Chinault, C. E. Sever, M. L. Slovak, C. L. Willman, and A. B. Deisseroth.** 1994. Consistent loss of the D5S89 locus mapping telomeric to the interleukin gene cluster and centromeric to EGR-1 in patients with 5q- chromosome. Blood **83:**199–208.
61. **Neuman, W. L., C. M. Rubin, R. B. Rios, R. A. Larson, B. M. Le, J. D. Rowley, J. W. Vardiman, J. L. Schwartz, and R. A. Farber.** 1992. Chromosomal loss and deletion are the most common mechanisms for loss of heterozygosity from chromosomes 5 and 7 in malignant myeloid disorders. Blood **79:**1501–1510.
62. **Passarge, E.** 1983. Bloom's syndrome, p. 11–21. *In* J. German (ed.), Chromosome mutation & neoplasia. Alan R. Liss, New York.
63. **Pedersen, B.** 1993. 5q-: pathogenetic importance of the common deleted region and clinical consequences of the entire deleted segment. Anticancer Res. **13:**1913–1916.
64. **Petes, T. D., R. E. Malone, and L. E. Symington.** 1991. Recombination in yeast, p. 407–521. *In* J. R. Broach, J. Pringle, and E. Jones (ed.), The molecular and cellular biology of the yeast *Saccharomyces*: genome dynamics, protein synthesis, and energetics, vol. I. Cold Spring Harbor Laboratory Press, Cold Spring Harbor, N.Y.
65. **Petrini, J. H. J., M. E. Walsh, C. Di Mare, J. R. Korenberg, X.-N. Chen, and D. T. Weaver.** 1995. Isolation and characterization of the human MRE11 homologue. Genomics **29:**80–86.
66. **Raymond, W. E., and N. Kleckner.** 1993. RAD50 protein of S. cerevisiae exhibits ATP-dependent DNA binding. Nucleic Acids Res. **21:**3851–3856.
67. **Robbins, J., S. M. Dilworth, R. A. Laskey, and C. Dingwall.** 1991. Two interdependent basic domains in nucleoplasmin nuclear targeting sequence: identification of a class of bipartite nuclear targeting sequence. Cell **64:**615–623.
68. **Roth, D. B., and J. H. Wilson.** 1988. Illegitimate recombination in mammalian cells, p. 621–654. *In* R. Kucherlapati and G. R. Smith (ed.), Genetic recombination. American Society for Microbiology, Washington, D.C.
69. **Saitoh, N., I. Goldberg, and W. C. Earnshaw.** 1995. The SMC proteins and the coming of age of the chromosome scaffold hypothesis. Bioessays **17:**759–766.
70. **Saltman, D. L., G. M. Dolganov, J. A. Warrington, J. J. Wasmuth, and M. Lovett.** 1993. A physical map of 15 loci on human chromosome 5q23-33 by two-color fluorescence in situ hybridization. Genomics **16:**726–732.
71. **Schiestl, R. H., J. Zhu, and T. D. Petes.** 1994. Effect of mutations in genes affecting homologous recombination on restriction enzyme-mediated and illegitimate recombination in *Saccharomyces cerevisiae*. Mol. Cell. Biol. **14:** 4495–4500.
72. **Sharples, G. J., and D. R. Leach.** 1995. Structural and functional similarities between the SbcCD proteins of Escherichia coli and the RAD50 and MRE11 (RAD32) recombination and repair proteins of yeast. Mol. Microbiol. **17:**1215–1217.
73. **Shen, Z., K. G. Cloud, D. J. Chen, and M. S. Park.** 1996. Specific interactions between the human RAD51 and RAD52 proteins. J. Biol. Chem. **271:**148–152.
74. **Shen, Z., K. Denison, R. Lobb, J. M. Gatewood, and D. J. Chen.** 1995. The human and mouse homologs of the yeast RAD52 gene: cDNA cloning, sequence analysis, assignment to human chromosome 12p12.2-p13, and mRNA expression in mouse testis. Genomics **25:**199–206.
75. **Shinohara, A., H. Ogawa, Y. Matsuda, N. Ushio, K. Ikeo, and T. Ogawa.** 1993. Cloning of the human, mouse, and fission yeast recombination genes homologous to *RAD51* and *recA*. Nat. Genet. **4:**239–243.
76. **Shinohara, A., H. Ogawa, and T. Ogawa.** 1992. Rad51 protein involved in repair and recombination in S. cerevisiae is a RecA-like protein. Cell **69:** 457–470.
77. **Stamato, T. D., R. Weinstein, A. Giaccia, and L. Mackenzie.** 1983. Isolation of cell cycle-dependent gamma ray-sensitive Chinese hamster ovary cell. Somatic Cell Genet. **9:**165–173.
78. **Taccioli, G. E., T. M. Gottlieb, T. Blunt, A. Priestley, J. Demengeot, R. Mizuta, A. R. Lehmann, F. W. Alt, S. P. Jackson, and P. A. Jeggo.** 1994. Ku80: product of the *XRCC5* gene and its role in DNA repair and V(D)J recombination. Science **265:**1442–1445.
79. **Taccioli, G. E., G. Rathbun, E. Oltz, T. Stamato, P. A. Jeggo, and F. W. Alt.** 1993. Impairment of V(D)J recombination in double-strand break repair mutants. Science **260:**207–210.
80. **Tavassoli, M., M. Shayeghi, A. Naism, and F. Z. Watts.** 1995. Cloning and characterization of the Schizosaccharomyces pombe rad32 gene: a gene required for repair of double strand breaks and recombination. Nucleic Acids Res. **23:**383–388.
81. **Thomas, K. R., and M. R. Capecchi.** 1987. Site-directed mutagenesis by gene targeting in mouse embryo-derived stem cells. Cell **51:**503–512.
82. **Thompson, L. H., K. W. Brookman, N. J. Jones, S. A. Allen, and A. V. Carrano.** 1990. Molecular cloning of the human *XRCC1* gene, which corrects defective DNA strand break repair and sister chromatid exchange. Mol. Cell. Biol. **10:**6160–6171.
83. **Valancius, V., and O. Smithies.** 1991. Double-strand gap repair in a mammalian gene targeting reaction. Mol. Cell. Biol. **11:**4389–4397.
84. **Verhaegh, G. W., W. Jongmans, B. Morolli, N. G. Jaspers, G. P. van der Schans, P. H. Lohman, and M. Z. Zdzienicka.** 1995. A novel type of X-ray-sensitive Chinese hamster cell mutant with radioresistant DNA synthesis and hampered DNA double-strand break repair. Mutat. Res. **337:**119–129.
85. **Walker, J. E., M. Saraste, M. J. Runswick, and N. J. Gay.** 1982. Distantly related sequences in the alpha- and beta-subunits of ATP synthase, myosin, kinases and other ATP-requiring enzymes and a common nucleotide binding fold. EMBO J. **1:**945–951.
86. **Weaver, D. T.** 1995. What to do at an end: DNA double-strand break repair. Trends Genet. Sci. **11:**388–392.
87. **Whitmore, G. F., A. J. Varghese, and S. Gulyas.** 1989. Cell cycle responses of two X-ray sensitive mutants defective in DNA repair. Int. J. Radiat. Biol. **56:**657–665.
88. **Zakharov, I. A., N. G. Suslova, and I. V. Fedorova.** 1983. Intragenic mitotic recombination induced by ultraviolet and gamma rays in radiosensitive yeast mutants. Genetika **19:**49–57.